Biomaterials and Biosystems 5 (2022) 100035

Contents lists available at ScienceDirect

Biomaterials and Biosystems

journal homepage: www.elsevier.com/locate/bbiosy

Development of decellularization protocol for caprine small intestine submucosa as a biomaterial

Hemant Singh [a], Shiv Dutt Purohit [a], Rakesh Bhaskar [b], Indu Yadav [a], Mukesh Kumar Gupta [b], Narayan Chandra Mishra [a,*]

[a] Department of Polymer and Process Engineering, Indian Institute of Technology Roorkee, Roorkee, Uttarakhand, India
[b] Department of Biotechnology and Medical Engineering, National Institute of Technology Rourkela, Rourkela, Odisha, India

ARTICLE INFO

Keywords:
Caprine small intestine submucosa
Decellularization protocols
Biomaterials
Tissue engineering
extracellular matrix

ABSTRACT

Decellularized animal tissues have been proven to be promising biomaterials for various tissue engineering (TE) applications. Among various animal tissues, small intestine submucosa (SIS) has gained attention of many researchers due to its easy availability from the abattoir waste, excellent physicochemical and biological characteristics of a good biomaterial. In this study, Caprine SIS was decellularized to get decellularized caprine SIS (DG-SIS). For decellularization, several physical, chemical and enzymatic protocols have been described in the literature. To optimize the decellularization of caprine SIS, several decellularization protocol (DP), including an in-house developed by us, had been attempted, and effect of the different DPs on the obtained DG-SIS were assessed in terms of decellularization, physiochemical and biological properties. All the DPs differ in terms of decellularization, but three DPs where ionic detergent like sodium dodecyl sulphate (SDS) has been used, largely affect the native composition (e.g. glycosaminoglycans (GAGs)), biological properties and other physiochemical properties of the G-SIS as compared to the DP that uses hypertonic solution of potassium iodide (KI) and non-ionic detergent (TritonX-100). The obtained DG-SISs were fibrous, hemocompatible, biocompatible, hydrophilic, biodegradable and exhibited significant antibacterial activity. Therefore, the DG-SIS will be a prospective biomaterial for TE applications.

1. Introduction

Tissue engineering is the set of techniques to develop bioartificial substitutes that are capable of repairing or regenerating damaged or diseased tissues and organs [1]. Most 'classical' TE involves using a scaffold in which living cells can be seeded to develop a viable tissue construct [1–3]. Scaffolds provide a three-dimensional biomaterial architecture that attempts to mimic the native extracellular matrix (ECM) and facilitate the attachment, proliferation, and differentiation of somatic and stem cells [4,5]. Several biomaterials, including metallic, ceramic, glass, and a large variety of polymers, have been tested and are routinely used for scaffold fabrications by many scientists [4,6–11]. More recently, decellularized tissues (e.g. heart, kidney, skin, SIS, liver, etc.) have emerged as potential natural biomaterials to replace synthetic biomaterials for generating engineered tissue [12–16]. Decellularized tissue offers several advantages over synthetic biomaterials in terms of biocompatibility, biodegradability and superior biological characteristics, similar to native ECM [17–19].

Decellularization of animal tissue involves several physical, chemical and enzymatic steps to break the cellular membrane, lyse the endogenous cells and remove the intracellular components from the tissue whereas preserving the native ECM [20–22]. A critical step in the decellularization of tissues is the set of zwitterionic, non-ionic or ionic detergents to dissociate and destabilize lipids, proteins and, DNA within the cells [20,21,23,24]. Ionic detergents such as sodium dodecyl sulphate (SDS) and sodium dodecyl cholate (SDC) are effective in cell elimination but might disturb the ECM structure and completely denature the proteins [25,26]. On the other hand, non-ionic detergents like Triton X100 (TX-100) are less harsh the ECM structure and keep the native protein [20,21]. Zwitterionic detergents such as 3-[(3-cholamidopropyl) dimethylammonio]-1-propane sulfonate (CHAPS) and tri-n-butyl-phosphate (TNBP) have shown good ECM ultrastructure preservation after decellularization, but confines in efficient cell removal [21,24,25]. Enzymatic treatment with exonucleases (e.g. Benzonase) and endonucleases (e.g. DNase) are commonly used to break the nucleotide bonds and remove remnant DNA [20,21,27]. Different tissue or organ types require different decellularization protocols, depending on their architecture and composition of ECM, and need to be optimized for respective tissue or organ before their intended use [24,28]. The effective decellularization protocol for specific tissue and organ also depends on various factors such as thickness (e.g. pericardium v/s dermis), tissue cellularity (e.g. tendon v/s liver), lipid content (e.g. brain

* Corresponding author.
E-mail address: narayan.mishra@pe.iitr.ac.in (N.C. Mishra).

https://doi.org/10.1016/j.bbiosy.2021.100035
Received 9 September 2021; Received in revised form 10 December 2021; Accepted 22 December 2021

v/s urinary bladder), fibre density (e.g. dermis v/s adipose tissue) etc. [24,29,30].

Among various animal tissues, small intestine submucosa (SIS) has been gaining high importance in TE applications because it can be obtained from the abattoir biowaste of slaughtered animals: thus, in one way, it will be economical and, in the other way, animal biowaste from an abattoir can be utilized for developing the value-added product, i.e., TE scaffold or device. Decellularized SIS (D-SIS) has been clinically validated for the reconstruction of different human organs, including lung [31], urethra [32] and vagina [33]. The D-SIS consists of natural biomolecules such as collagen, integrin proteins and, various glycosaminoglycan (GAGs), including heparin, hyaluronic acid and chondroitin sulfate etc.) [13,34,35], which support cellular growth to accelerate tissue repair/ and regeneration [34–36].

The use of D-SIS in TE offers the advantage that it can be obtained from xenogeneic species (e.g. porcine, bovine, and ovine) for human TE applications [37–40]. Among various xenogeneic species, porcine and bovine D-SIS has been the most studied. However, bovine and porcine D-SIS pose a high risk of zoonotic disease transmission (e.g., H1N1 virus, bovine spongiform encephalitis etc.) to humans besides potential immunological reaction [5,34,35]. Goats (caprine; *Capra aegagrus hircus*) are also prone to a special kind of transmissible disease, i.e. scrapie. The prions associated with scrapie do not cause any diseases to humans [41,42]. Apart from this, Vaccari et al. [43] have pointed out that the occurrence of scrapie is very low in goats compared to other cattle. The literature also mentioned that no cases of scrapie were observed in the goats throughout Indian subcontinents [42,43]. Thus, it indicates that goat tissue-based decellularized biomaterial could be a safer option for TE applications as compared to bovine, porcine and ovine tissues. Goat liver and skin-based decellularized ECM were already explored for TE applications, which showed the antibacterial, biocompatible and non-immunogenic properties [44,45]. Furthermore, goats are widely available in South Asian countries. According to the Agricultural and Processed Food Products Export Development Authority (APEDA), India is the largest producer and exporter of goat meat in 2020-21 [46]. Processing of goat for meat in the abattoir produces biowaste in the form of the small intestine (G-SI). Thus, biowaste from caprine abattoir was utilized to develop a value-added product. However, even though caprine tissue may be a better option for SIS source, the least attention has been given to utilizing caprine SIS (G-SIS) for TE applications.

For decellularization, several physicals, chemical and enzymatic protocols have been described in the literature. The optimized protocol for G-SIS has not yet been investigated in the literature. In this study, to optimize the decellularization of G-SIS, several decellularization protocols (DP), including a new one developed by us, had been attempted. The effect of different DPs on caprine SIS was assessed in terms of decellularization, physiochemical and biological properties. The first three protocols (DP1, DP2 and DP3) have been previously utilized to decellularize ovine and porcine SIS [15,37,40]. The fourth protocol (DP4) was in-house developed in this study by combining the advantageous components of various DPs.

2. Materials and methods

2.1. Materials

Fresh G-SI was collected from a local caprine slaughterhouse of Saharanpur, India. Sodium chloride (NaCl), methanol, chloroform, ethanol, TX-100, chondroitin sulphate, potassium iodide (KI), hydrogen peroxide (H_2O_2), fluorescein diacetate (FDA) and ethidium bromide (EtBr) stains were purchased from Sigma-Aldrich (MO, USA). Phosphate buffer saline (PBS), ethylenediaminetetraacetic acid (EDTA), trypsin, sodium dodecyl sulphate (SDS), antibiotic solutions, Hematoxylin and Eosin (H&E) stain, collagenase enzyme, Dulbecco's modified Eagle medium (DMEM), DNA extraction kit, 3-(4,5-dimethylthiazol-2-yl)-2,5-diphenyltetrazolium bromide (MTT) assay kit, alcian blue, 1, 9-dimethyl-methylene blue (DMMB), Mueller-Hinton (MH) agar, MH) broth, papain were purchased from Himedia (Mumbai, India). Double distilled and deionized water was used throughout the study.

2.2. Isolation of G-SIS

Fresh G-SI was transported, in an insulated box having PBS with the antibiotic solution 100X liquid, HiMedia (mixture of penicillin and streptomycin) at 4°C temperature, to the laboratory within 4 h of the collection after washing with water to remove the intestinal waste content. The antibiotic solution was used to inhibit the growth of the microbes which may be present in the G-SI, or may come from the environment, to avoid the deterioration of G-SI, if any. A soft scrubber removed the mucosal layer of G-SI, and muscularis externa and serosa layers were mechanically peeled off with the help of a knife to obtain the G-SIS. Finally, the isolated G-SIS was fragmented into pieces of 10 cm length for further study [15].

2.3. Decellularization of the G-SIS

In the quest for a suitable protocol for G-SIS decellularization—four different DPs were employed, as shown in (figure 1). Among all the DPs, three DPs (DP1, DP2 and DP3) were adapted from previous literature [15,37,40], while the DP4 was developed by considering the advantageous components of the different protocols. Earlier, the DP1-3 had been applied for various tissue sources, such as porcine and ovine SIS, but in this study, the protocols were applied to decellularize caprine tissue source, G-SIS.

2.3.1. DP1

The G-SIS was immersed in the saline solution for 48 h followed by chemical treatment (0.05% SDS for 6 h and 0.1% TX-100 for 3 h) and physical treatment (agitation at 100 rpm, temperature at 37°C). After each treatment, the G-SIS was rinsed with distilled water for 90 min (30 min for 3 times) [40].

2.3.2. DP2

The G-SIS was submersed in degrease solution (methanol/chloroform, 1:1 v/v) for 12 h and washed 3 times in deionized water, followed by enzymatic digestion (0.05% trypsin/0.05% EDTA) at 37°C for 12 h and thereafter washed 3 times in saline solution. Finally, the G-SIS was incubated at 37°C in detergent (0.5% SDS) in 0.9% sodium chloride solution for 4 h and washed 3 times in saline solution [15].

2.3.3. DP3

Here, the protocol described by Syed et al. [37] was modified in terms of perfusion to the immersion/agitation method. The G-SIS was initially treated with 1% solution of SDS for 12 h and thoroughly rinsed with deionized water, followed by washing (through agitation) for 15 min with deionized water and then incubating in 1% solution of TX-100 for 30 minutes. Finally, the G-SIS was rinsed by agitation in deionized water for 30 min. All the steps were performed at room temperature (RT, 30°C) and with agitation (100 rpm).

2.3.4. DP4

The G-SIS was incubated in 1.0 M of KI solution for 24 h (after 8 h, KI solution was changed), followed by a mild non-ionic detergent (0.1% TX-100 in deionized water) for 24 h. After each step, the G-SIS was rinsed with deionized water for 90 min (30 min for 3 times). All of the process steps were carried out at 4°C with mechanical treatment (agitation at 150 rpm).

After completion of DP1-4, DG-SIS samples were sterilized by rinsing in ethanol/H_2O_2 [70% (v/v) ethanol + 0.1% (v/v) H_2O_2] solution for 2 h, followed by washing through distilled water, to eliminate the remaining sterilization solution. For further analysis, all the DG-SISs samples

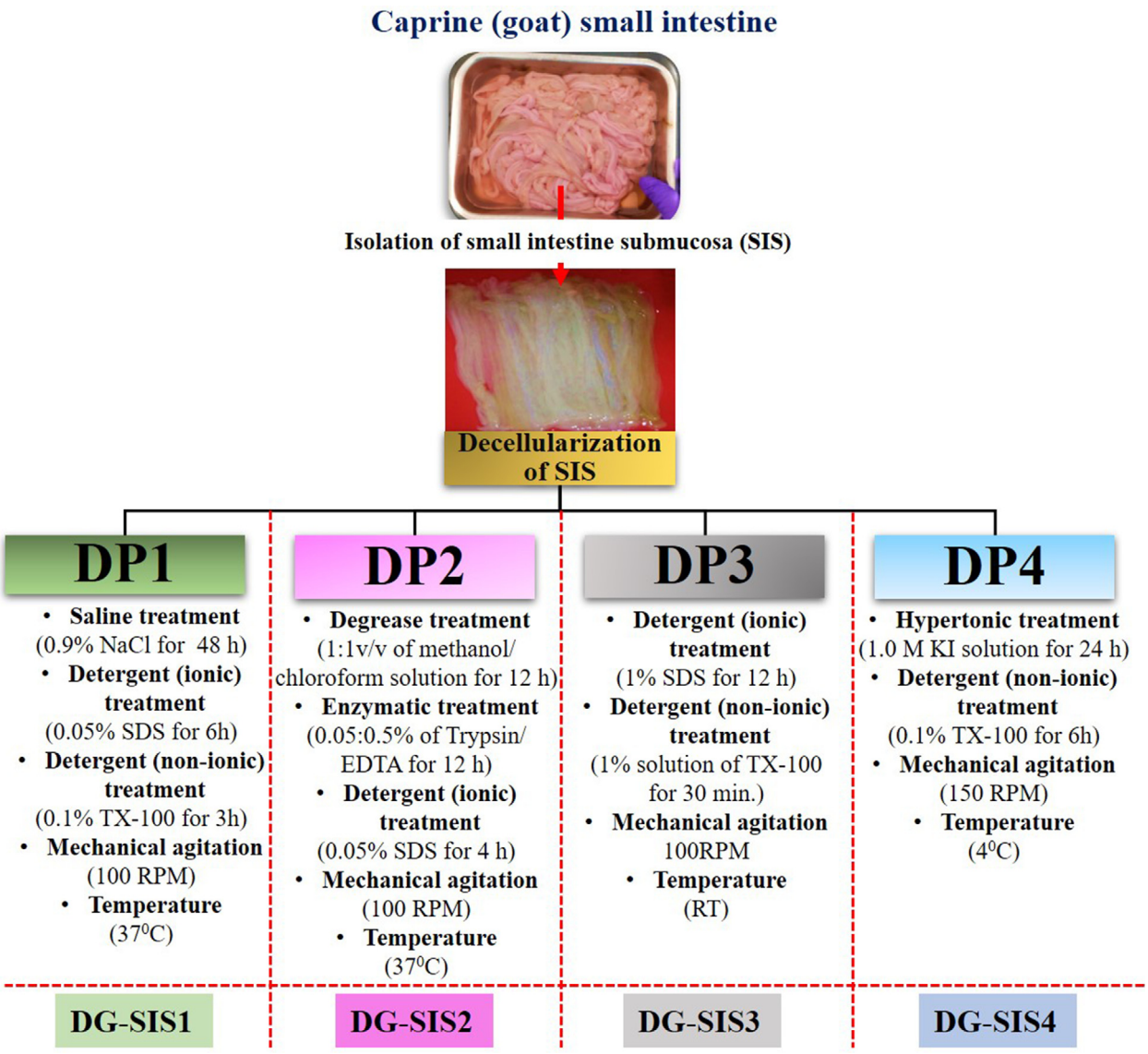

Fig. 1. Systematic diagram of an overview of decellularization protocols for G-SIS.

were lyophilized, sterilized again by using UV light (256 nm) for 60 min (30 minutes on each side), and then packed in Ziplock bags, and stored at 4°C.

2.4. Sterility verification

The sterility of the DG-SISs, before being used for research analysis, was verified by following the protocol as described by Sweta et al. [13]. The DG-SISs (n=3 per sample) were briefly incubated in the DMEM nutrient media at 37°C in the CO_2 incubator. The absence of any turbidity, after 15 days, in the media indicates the sterility of the DG-SISs.

2.5. Verification of decellularization

2.5.1. DNA quantification

DNA quantification was performed to determine the presence of DNA content in the G-SIS and DG-SISs and evaluate the efficiency of the DPs. Briefly, the total DNA content present in the 1 g of dry samples (n=3 per sample) was isolated and purified by following the protocol suggested by the manufacturer (HiPurA^{TM} Mammalian Genomic DNA Purification Kit, HiMedia). The collected DNA was quantified by UV-Vis spectrophotometry (Eppendorf Biophotometer, Germany) at 260 nm.

2.5.2. Histological assessment

Histological study (Hematoxylin & Eosin staining) of the G-SIS and DG-SISs (n=3 per sample) was performed to evaluate the efficacy of the DPs qualitatively. Hematoxylin is a positively charged basic stain that binds negative-charged nucleic acids and stains purple/dark blue. Eosin is a negatively charged acidic stain, which binds positively charged biomolecules (amino acids) present in the ECM and stains them pink. Histological study was performed following the protocol steps, i.e., fixation, H&E staining, mounting, and image visualization by a microscope, as described by Sweta et al. [13].

The effect of DPs on G-SIS, in terms of proteoglycan content, was measured by Alcian blue staining protocol as reported previously [30]. Briefly, samples (n=3) were stained with Alcian blue stain for 30 min and counterstained with the nuclear fast red solution for 1 min. Images were taken by using a 40X magnification light microscope, and the intensity of the staining of proteoglycans was quantified using Image J analysis software (ImageJ, National Institute of Health, USA)

2.6. GAG quantification

The effect of DPs on the GAG content in the G-SIS was evaluated by the DMMB assay as described by Farndale et al. [47]. Briefly, a solution

of 125 mg/ml papain, 5 mM cysteine-HCl, and 5 mM disodium EDTA in PBS was prepared. Then, 10 mg of lyophilized samples (n=3 per sample) were dissolved in the prepared solution. 50 µl of each sample was mixed with 250 µl DMMB in a well microtiter plate, and the optical density values were taken out by UV-Vis spectrophotometer at 530 nm. The GAG content in the samples was determined by reference to a standard curve prepared using different concentrations of chondroitin sulphate sodium salt.

2.7. Scanning electron microscopy

Surface morphology and integrity of the lyophilized G-SIS and DG-SISs were analyzed using Field Emission Scanning Electron Microscope (FESEM, MIRA3TESCAN, Czech Republic) at an operating voltage of 5 kV and a working distance of 5 mm. To evade the electron charging, each sample was sputter-coated with gold prior to the FESEM analysis [8].

2.8. Swelling behaviour

The swelling behaviour of the samples was determined by the following protocol as described previously [4]. Briefly, the lyophilized samples (n=6 per sample) were immersed in the PBS solution at 37°C and then measured samples' weight at every 30 min time intervals. The experiment was performed until the equilibrium point of swelling of samples was obtained, where no further swelling of the samples was observed. Then, swelling percentage (S%) was calculated as per equation 1.

$$S\% = \frac{Ws - Wd}{Wd} X 100 \quad (1)$$

Where W_s = weight of wet samples after swelling, and W_d = weight of the samples after drying.

2.9. In vitro *biodegradation study*

The biodegradation of the lyophilized G-SIS and DG-SISs was evaluated enzymatically and in absence of enzyme, by following protocol as described previously [35]. A solution containing approximately 0.0625 U/mL of collagenase enzyme Type-I (HiMedia Laboratories Pvt. Ltd, India) was prepared in PBS solution. For enzymatic degradation study, 1 mg of samples were weighed and immersed in 10 ml of collagenase enzyme solution. Under the non-enzymatic condition, samples were immersed in 10 mL of PBS. All samples (n = 3 per sample) were incubated at 37°C in an incubator shaker. To determine the degradation profile, the samples were removed from degradation solutions at regular time intervals. Afterwards, samples were thoroughly washed with distilled water and dried. Further, each sample was weighed, and the *in vitro* degradation was calculated as per equation 2.

$$Weight\ loss(\%) = \frac{w_o - w_t}{w_o} \times 100 \quad (2)$$

Where W_0 denotes the initial weight of the samples and W_t denotes the weight of the degraded samples at different time intervals.

2.10. Mechanical properties

The thickness of the wet G-SIS and DG-SISs was manually recorded as an average of 10 measurements (n=10 per sample) by using the digital micrometre (Insize-code: 3109–25). Tensile tests were performed using a universal testing machine (Instron 5566, USA). Samples were placed between the clamps of the testing device and pulling was performed with a strain rate of 5 mm/min. Stress versus strain graphs of each sample was used to calculate the samples' mean ultimate tensile strength (UTS) and e-modulus.

2.11. Evaluation of bacterial growth on DG-SISs

Bacterial growth on DG-SISs was evaluated by a protocol described by Gupta et al. [44]. In brief, *E. coli* (gram-negative *Escherichia coli)* and *S. aureus (*gram-positive *Staphylococcus aureus)* strains were streaked on MH agar plates. In addition, 10 ml of MH broth was inoculated with isolated colonies and incubated at 37°C overnight. These cultures were collected from MH broth and diluted to 5×10^5 CFU/mL. After that, 100 µL of bacterial suspension was transferred to a 96-well culture plate: all the controls and DG-SISs solutions were prepared as described in the study conducted by Gupta et al. [44] Then, the prepared DG-SIS solutions (25µL) were added to the bacterial solutions to assess their antibacterial activity and absorbance (570 nm) was measured at different predetermined time intervals. All the assays were performed in triplicates to check the reproducibility of the results.

2.12. In vitro hemocompatibility assessment

Hemocompatibility (blood cell compatibility) of the samples was carried out by following the protocol described by Fan et al. [48]. Briefly, fresh blood was collected in an anticoagulant tube and diluted 2 % by NaCl. One gram of each DG-SIS sample (n=3) was soaked in saline for 24 h to get the sample extract. The sample extract was then mixed in the diluted blood and incubated at 37°C temperature. After 4 h, the samples were centrifuged (1500 rpm) for 10 minutes and measured the OD value of each sample using a spectrophotometer at an absorbance of 545 nm. Hemolysis (%) was assessed by using the OD values with the following equation 3.

$$\%\ \text{Hemolysis} = \frac{\text{OD(treated)} - \text{OD(}-\text{ve control)}}{\text{OD(+ve control)} - \text{OD(}-\text{ve control)}} \text{x } 100\% \quad (3)$$

According to the ASTM F756, materials are considered hemolytic when % hemolysis >5%; slightly hemolytic at % hemolysis between 2 to 5%, and non-hemolytic for % hemolysis <2%.

2.13. In vitro cytotoxicity assessment

For in vitro cytotoxicity assessment, a mouse fibroblast L929 cell line was purchased from NCCS, Pune and sub-cultured in DMEM media solution at 37°C in the CO_2 incubator. Sterilized 1 cm^2 pieces of DG-SISs (n=3 per sample) were kept in the CO_2 incubator along with complete media for 12 h. After that, cells were seeded at the density of 5,000 cells/cm^2 over the DG-SISs in each well-plate. Finally, culture plates were incubated in an incubator with 5% CO_2 supply at 37°C. Every alternate day, the media was changed, and cells were examined under the optical microscope [35,44]. Cells cultured on tissue culture plates (TCP) were taken as a control for comparison.

For calculating the cell attachment, samples were trypsinized at a fixed time interval (2 h, 5 h, and 8 h), and the cell numbers were calculated with a cell counter. The DG-SISs (n=3 per sample) were also evaluated for their cytotoxicity in terms of cell viability and proliferation potential of L929 cell line by colourimetric MTT after 1, 3, and 5 days of culture at 37°C in the CO_2 incubator. After cell seeding, samples were washed with PBS and incubated in yellow MTT dye for 4 h in the CO_2 incubator. Then, aliquots were pipetted out, and a solubilization buffer was added to dissolve the formazan crystals. The optical density values of each well of the culture plate were calculated at 570 nm by a microplate reader. FESEM visualized cell adhesion over the DG-SISs after 5 days of the cell culture as described previously [35]. Briefly, cell-seeded DG-SISs constructs were fixed with glutaraldehyde and dehydrated with ethanol (60%, 80%, 90%, and 100%). Finally, the cells on the DG-SISs were visualized under the FESEM.

FDA/EtBr (fluorescein diacetate/ethidium bromide) assay was performed to visualize the cell viability and determine the live/dead cells percentage on the DG-SISs matrices as explained earlier [35]. Briefly, matrices were stained with 10 μM FDA (live cells stained in fluoresce

green) and 25 μM of EtBr (dead cells stained in fluoresce red) on 5 days of culture. After 5 min, stained matrices were observed under the Olympus fluorescence microscope. Fluorescent images were further processed with ImageJ software to determine the live/dead cells percentage over the DG-SISs matrices.

2.14. Statistical analyses

Non-parametric (Kruskal–Wallis) statistical analysis was performed for a small number of data groups (n=3), but an analysis of variance (ANOVA) and a t-test had been done for a large number of data groups (n=10). Origin 8.9 and Microsoft Excel had been used for statistical analysis. Differences were considered statistically significant at $p < 0.05$.

3. Result

3.1. Verification of DPs efficiency in terms of DNA content

Figure 2A shows that all the DPs were able to significantly reduce the DNA content of G-SIS (411.19 ng per mg of the dry weight of tissue) in all the DG-SIS samples. The DNA content in the DG-SIS1, DG-SIS2, DG-SIS3, and DG-SIS4 was 23.86, 25.68, 27.35, 21.84 ng/mg of the dry weight of tissue, respectively. However, no significant difference was observed among all the DPs in terms of available DNA contents in all the DG-SIS matrices.

3.2. Effect of DPs on GAG and proteoglycans content of the DG-SISs

The GAG content in the DG-SIS1, DG-SIS2, DG-SIS3 and DG-SIS4 was 7.18, 6.45, 5.32, and 8.17 μg GAG/mg dry weight, respectively, while in the G-SIS it was 14.1 μg GAG/mg dry weight (Figure 2B). The GAG content in DG-SIS4 was highest among all the DG-SISs. Percentage of proteoglycans content (Figure 2C) in the DG-SIS3 was significantly reduced, while no statistical difference was observed in the DG-SIS1, DG-SIS2 and DG-SIS4, as compared to the untreated G-SIS.

3.3. Swelling behaviour of DG-SISs

Swelling behaviour (Figure 2D) indicates that all the samples (DG-SIS1, DG-SIS2, DG-SIS3 and DG-SIS4) are almost fully hydrated in about 60 min, although there is a slight increment of swelling after 60 min. The maximum percentage swelling was 878, 663, 604, 493, and 765 respectively for the samples of the G-SIS, DG-SIS1, DG-SIS2, DG-SIS3 and DG-SIS4.

3.4. In vitro *biodegradation of DG-SISs*

In vitro biodegradation study showed that the G-SIS and DG-SIS matrices were biodegradable (Figure 2E, F). Furthermore, under enzymatic conditions (collagenase enzyme Type-I), the G-SIS and DG-SIS matrices showed complete weight loss within 144 h (Figure 2E). In contrast, under non-enzymatic conditions (PBS), the G-SIS and DG-SIS matrices showed complete weight loss within 65 days (Figure 2F). But, a slight fluctuation in weight loss occurred among all the DG-SIS matrices at various time intervals.

3.5. Verification of DPs efficiency in terms of histological analysis

Histological analyses of the cross-section of matrices are shown in Figure 3A. In the H&E-stained image of cross-sectioned G-SIS, black arrows showed the presence of cells. However, after decellularizing G-SIS by all the DPs depicted the absence of cellular nuclei/components stain (blue/purple) in all the DG-SIS matrices. H&E stained images were also visualized (pink coloured) the collagen fibers in the DG-SIS matrices, and the available proteoglycan content was visualized in Figure 3B.

Table 1
Thickness and mechanical properties (Mean±SD) of G-SIS and DG-SISs matrices.

Groups	Thickness (μm)	UTS(MPa)	E-Modulus (MPa)
G-SIS	37.20±3.20*	10.10±3.45*	56.05±6.21*
DG-SIS1	19.01±4.10	4.03±0.97	24.67±6.42
DG-SIS2	21.60±2.40	5.12±0.99	32.67±13.05
DG-SIS3	17.33±2.76	3.68±0.89	28.34±4.47
DG-SIS4	22.97±3.77	5.90±0.96	38.22±10.10

Here, * $p<0.05$ was considered as a significant difference.

Furthermore, the transversal section of matrices was also histologically analyzed, as shown in supplementary information 1.

3.6. Surface morphology and integrity of DG-SISs

The surface morphology and integrity of the cross-sectioned matrices was visualized by FESEM images (Figure 3C). FESEM image of the G-SIS showed a protected layer compared to the DG-SIS matrices. However, after DPs, all the DG-SIS matrices showed the presence of fibres with varying diameters, and a protected layer of G-SIS was removed. The fibrous morphology of the DG-SIS matrices was also in accordance with the H&E stained images (Figure 3A) visualized (pink colour) the collagen fibers in the DG-SIS matrices. The transversal section of matrices was also visualized by FESEM images, as shown in supplementary information 1.

3.7. Mechanical properties of DG-SISs

The thickness of DG-SISs ranged between 17.33 to 22.97 μm (Table 1) and was significantly less than the G-SIS (37.20 μm). Table 1 depicted that the UTS and E-modulus of the DG-SISs were considerably lower than the G-SIS.

3.8. Short-term antibacterial property in DG-SISs

Evaluation of bacterial growth (*E. coli* and *S. aureus)* on DG-SISs revealed that the digested solutions of all the DG-SIS matrices possessed short term antibacterial activity against both the bacteria (Figure 4A, B). The DG-SIS matrices showed effective growth inhibition of the *E. coli* up to 25 h (Figure 4A) and *S. aureus* up to 15 h (Figure 4B). There was no significant difference in the antibacterial activity among the DG-SIS matrices. Small variations in antibacterial activity (growth inhibition time) of different DG-SIS matrices was observed against *E. coli* and *S. aureus.*

3.9. In vitro *hemocompatibility of DG-SISs*

Hemocompatibility (Figure 4C) of the DG-SIS extracts showed no rupture of erythrocytes in the tubes, whereas the erythrocytes were ruptured in the positive control, as indicated by the reddish appearance of the supernatant, implying full-scale hemolysis. The hemolysis (%) was measured as 1.20 for DG-SIS1, 1.81 for DG-SIS2, 2.13 for DG-SIS3, 0.79 for DG-SIS4 (Figure 4C). Further, the hemocompatibility analysis was performed on the DG-SIS matrices in sheet form. The results for DG-SIS matrices in sheet form are provided in supplementary information 2.

3.10. In vitro *cytocompatibility and cellular behaviour on DG-SISs*

All the matrices were found to support the L929 cell attachment (Figure 4D). The percentage of cell attachment over the matrices was significantly increased with the increase of the duration of culture as compared to control (TCP). Cell proliferation and viability over the DG-SIS matrices were very good, as evidenced by the high absorbance value in MTT assay with L929 mouse fibroblast cells (Figure 4E). After 5 days of culture, DG-SIS4 shows the highest cell growth (Figure 4E). FESEM

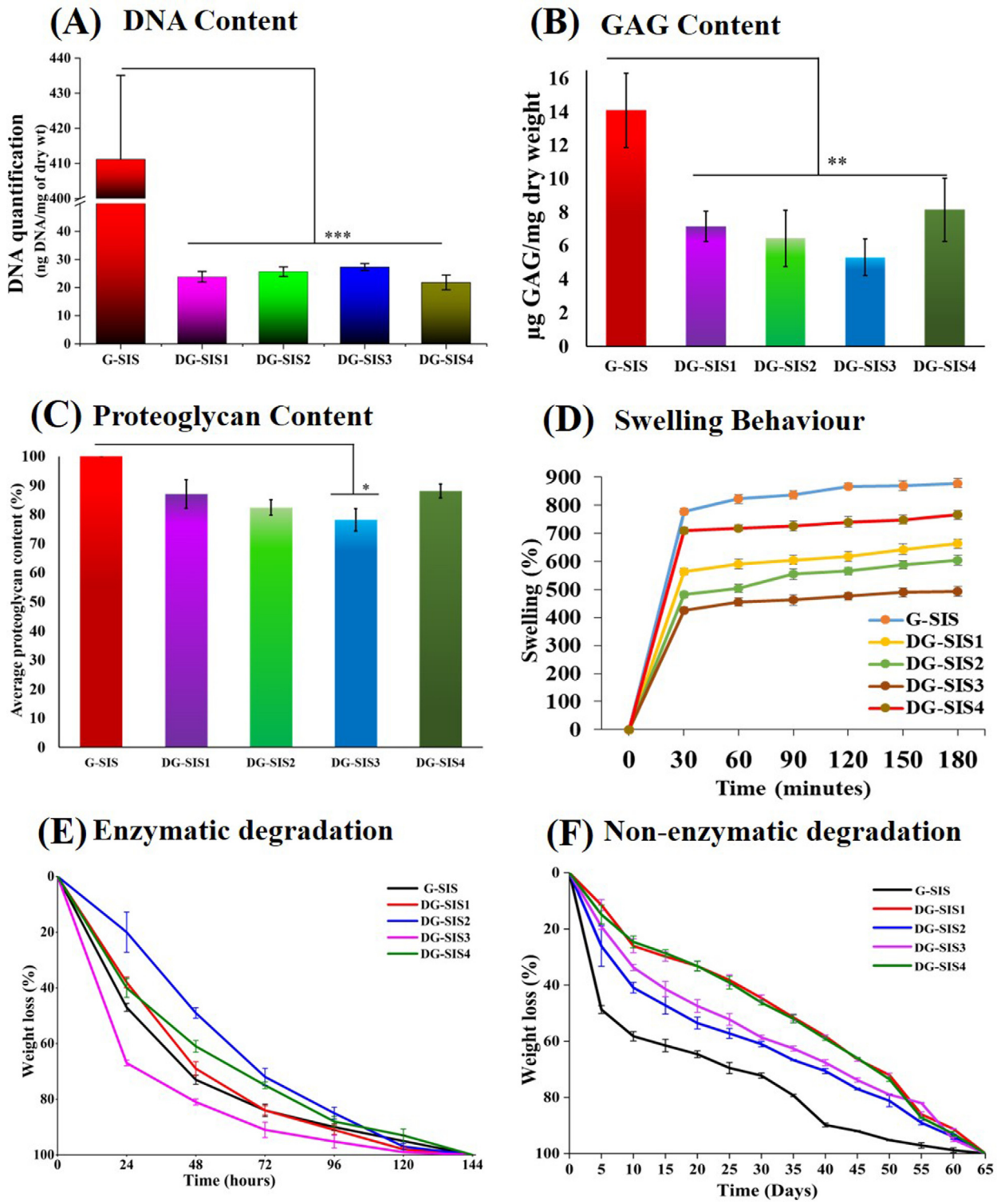

Fig. 2. (A) Evaluation of the DPs efficiency in terms of DNA content, (B) GAG content, (C) proteoglycans content, (D) swelling behaviour, (E) in vitro biodegradation of the matrices under enzymatic conditions, and (F) in vitro biodegradation of the matrices under non-enzymatic conditions. Means and standard deviations are shown by columns and error bars. Here, a significant difference was considered as * $p<0.05$.

images in (Figure 4G) depict good cell adherence and proliferation over the decellularized DG-SIS matrices after 5 days of cell culture. Figure 4H shows the live/dead cells over the DG-SIS matrices after 5 days of culture. All matrices show maximum green coloured live cells compared to a few red coloured dead cells. Further, Figure 4F depicted the live/dead cells percentage over the matrices after 5 days of culture. The outcomes indicate all matrices are compatible with L929 fibroblast cells. However, the percentage of dead cells was significantly higher over the DG-SIS3 compared to DG-SIS4. These results have supported the outcome of the MTT assay (figure 4E).

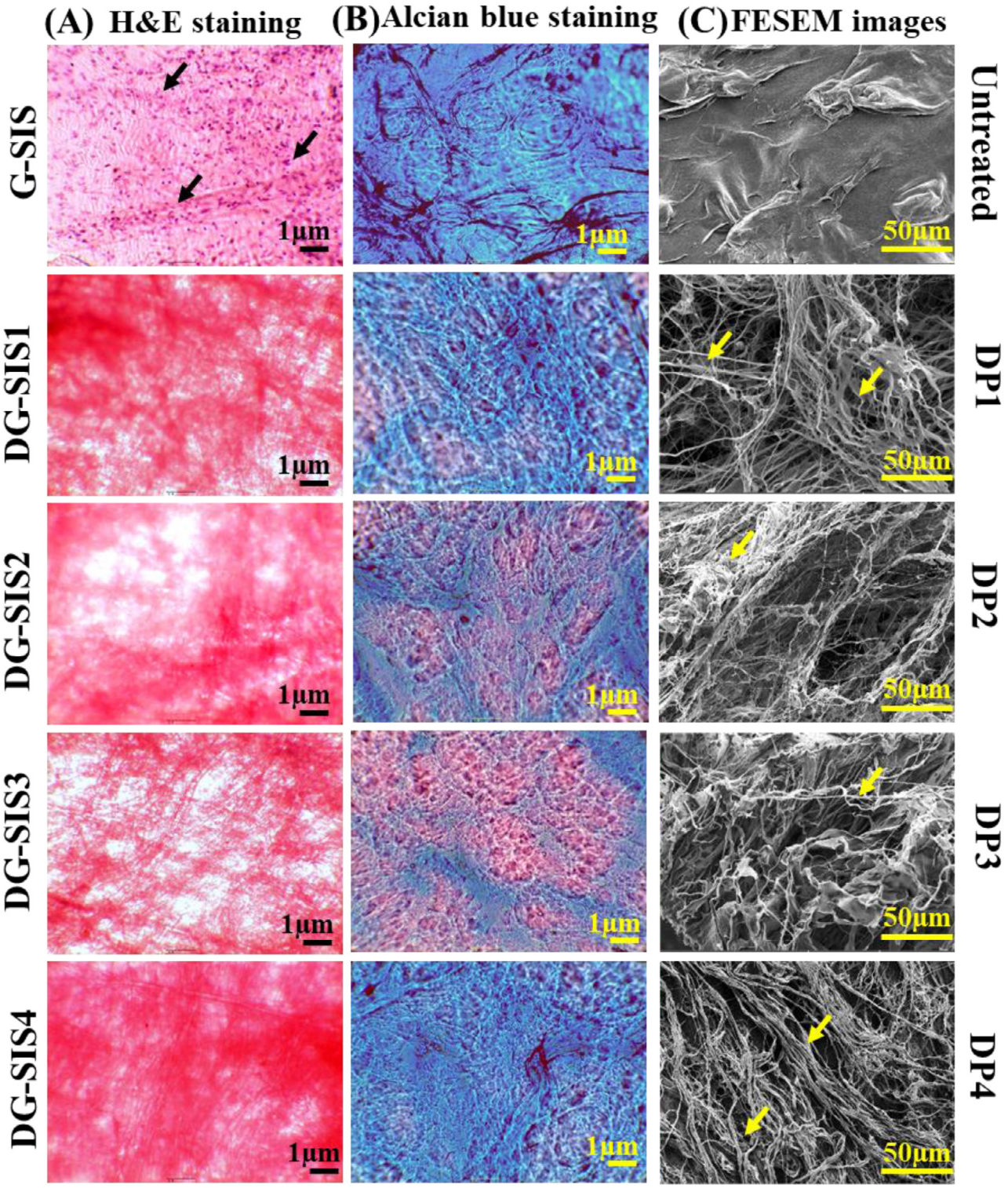

Fig. 3. (A) Evaluation of the DPs efficiency in terms of histological analysis (H&E staining; black arrows indicate the presence of cells), (B) alcian blue staining showing the available proteoglycan content and (C) FESEM images showing the surface morphology of the G-SIS and DG-SISs; yellow arrows indicate the presence of fibres.

4. Discussion

The SIS is extensively employed for tissue repair and regeneration due to the benefits provided by its functional components of ECM [5, 19]. However, SIS could trigger adverse immune responses elicited by intrinsic cells' genetic material and epitopes [5, 34, 35]. Thus, eliminating intrinsic cells from SIS must be required to minimise unfavourable immunogenic responses before being transplanted into the body. Decellularization is a suitable technology to eliminate the intrinsic cells from SIS [21, 23, 24]. Different tissues or organ types require different decel-

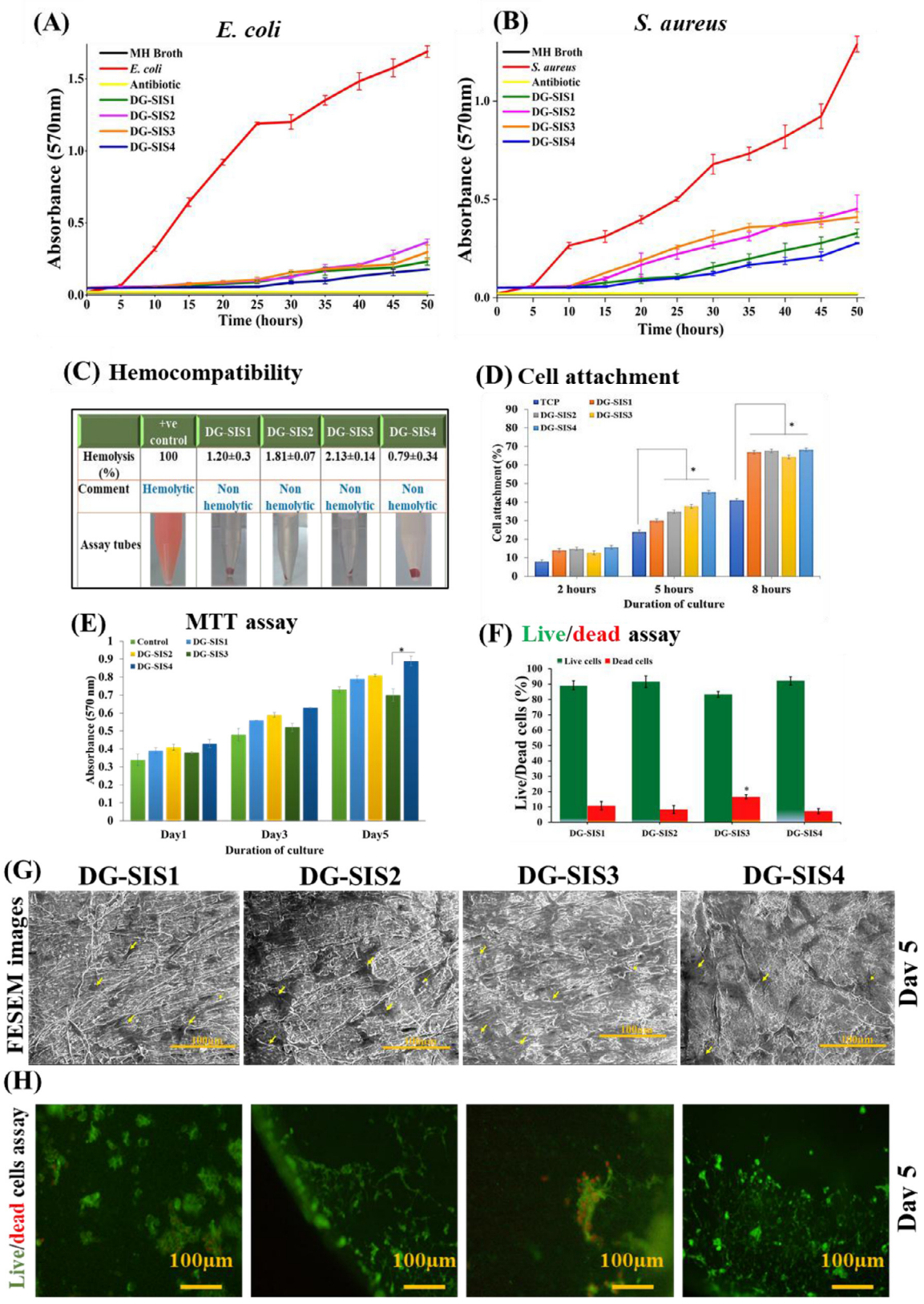

Fig. 4. (A) Short-term antibacterial activity of DG-SIS samples against *E. coli.*, (B) Short-term antibacterial activity of DG-SIS samples against *S. aureus*, (C) hemocompatibility of the DG-SIS matrices, (D) cell attachment, (E) cell proliferation, as measured by MTT assay, (F) live and dead cells percentage on the G-SIS and DG-SISs matrices, (G) FESEM images of cells attached to DG-SISs, and (H) live and dead cells over the G-SIS and DG-SISs. Means and standard deviations are shown by columns and error bars. Here, * $p<0.05$ was considered as a significant difference.

lularization protocols, depending on their architecture and composition of ECM [24, 28]. Thus, it is important to develop the most appropriate protocol for specific tissue decellularization while retaining the ECM components and bioactive compounds when eliminating the resident cell [24, 27].

In the quest for a suitable decellularization protocol for caprine SIS, this study employed four different protocols. The first three protocols (DP1, DP2 and DP3) have been previously utilized to decellularize ovine and porcine SIS [15,37,40], while the DP4 was in-house developed by considering the advantageous components of the different protocols. The effect of protocols on caprine SIS was comparatively assessed in terms of decellularization, physiochemical, and biological properties.

Thus, if the available DNA content in the decellularized tissues is less than 50 ng/mg dry weight of the sample, the undesirable host immune response will be prevented after implantation [13]. In this study, all the DPs efficiently reduced the less than 50 ng of DNA content per mg dry weight of all the DG-SIS matrices. This indicates that all the DPs were efficient for decellularizing the G-SIS. Rashtbar et al. used the DP1 for decelluarization of ovine SIS, which efficiently reduced DNA content from ovine SIS [40]. DP2 and DP3, for porcine SIS, also depicted significantly reduced intrinsic DNA content from the porcine SIS [15, 37].

After decellularizing caprine SIS by all the DPs, absence of cellular components stain (blue/purple) was observed in all the DG-SIS matrices. This indicates that all the DPs were capable of decellularizing the caprine SIS successfully. H&E stained images of all the DG-SIS matrices also shoowed negligible DNA content in the DG-SIS matrices. Decellularized goat-lung, porcine SIS and ovine-SIS based ECM matrices also showed similar outcomes [13,37,40]. H&E stained images visualized (pink coloured) the collagen in the DG-SIS matrices, as observed by other researchers in other tissues [44].

Preservation of non-fibrillar elements (GAG, proteoglycans) of caprine SIS was also an essential requisite for DPs. Non-fibrillar elements play an important role in cell-cell interaction, cell adhesion, survival, migration, proliferation, and maintaining the tissue's 3D structure and hydration level [30]. The GAG content in DG-SIS4 was the highest among all the DG-SISs, because DP4 (KI, TX100 and low temp.) depleted less GAG content than other DPs involving SDS. Thus, DP4 appears to be a better protocol than DP1-3 for decellularizing G-SIS, to preserve the GAG and proteoglycans content. The higher GAG and proteoglycans content in the DG-SIS may provide better cell attachment, proliferation and maturation [30,40]. Similar results were also observed for porcine and ovine SIS by other researchers [15,30,40].

Moreover, biomaterials should be hydrophilic and can be vital in retaining body fluids and supplying nutrients to the cells, essential for tissue engineering application [4, 35]. All the fabricated DG-SIS matrices were highly hydrophilic, but differences in swelling may be due to variation in caprine SIS's available ECM components (e.g., GAG and proteoglycan). The hydrophilic characteristic of biomaterials aids cell growth, as previously reported works of the literature [4, 35].

The ideal biomaterial should have suitable biodegradability for tissue engineering applications [8, 35]. The decellularized caprine SIS is biodegradable. But, a slight fluctuation in weight loss occurred among all the DG-SIS matrices at various time intervals: this might be due to the varying GAG and proteoglycans content. It may also be due to the disruption between the fibre-fibre bonding. All the DG-SIS matrices showed the presence of fibres with varying diameters after G-SIS decellularization. The fibrous morphology of the DG-SIS matrices was also in accordance with the H&E stained images visualized (pink coloured) the available collagen in the DG-SIS matrices. Fibrous morphology of the decellularized caprine SIS was similar to D-SIS of the porcine, bovine and ovine SIS as described earlier [15,30,37,40].

The reduction in thickness of the DG-SIS may be due to the reduced amount of ECM content (e.g., glycoproteins and proteoglycans) and the absence of cells in the DG-SISs that consequently affected the swelling behaviour, mechanical strength, and degradability of the DG-SISs. Further, the difference in thickness among the DG-SISs could be due to the difference in the DPs. Furthermore, the decellularized caprine SIS thickness is very thin and translucent compared to porcine and bovine SIS. In previous studies, the thickness of the different decellularised tissues ranged between 50 to 220μm in porcine SIS [49] and 15.83 to 20.33μm in ovine SIS [40]. The difference between the caprine SIS, porcine SIS and ovine SIS may be due to the differences in protocol and/or origin and age of the source. The difference in the mechanical properties may arise from the origin, age of source tissue and the difference in the DPs [40]. DPs, employing SDS and enzymes, significantly reduce mechanical strength through the collagen fibres' misalignment and reduction of the ECM (e.g., collagen, proteoglycans, and glycoproteins) content in the DG-SIS. In earlier studies, the tensile strength of different acellular tissues was reported to be 7.2 MPa for Porcine DG-SIS [49] and 2.91 to 6.27MPa for ovine DG-SIS [40].

In vitro collagenase enzyme-mediated degradation of DG-SISs has been used as a model for indicating the antibacterial effects of available peptides in the degradation products of DG-SIS. There was no significant difference in the antibacterial activity among the DG-SIS matrices. Small variations in antibacterial activity (growth inhibition time) of different DG-SIS matrices against *E. coli* and *S. aureus* may be due to the differences in the thickness of the bacteria's cell wall and/or defence mechanism. The short-term antibacterial property of the DG-SIS matrices may be due to the presence of naturally occurring antibacterial peptides (ABPs) produced due to the degradation of DG-SIS matrices [44, 50]. However, it is unknown whether they are the same as already identified ABPs or different ABPs. Gupta et al. showed the short-term antibacterial properties of the decellularized goat lungs matrix against *E. coli* for up to 9 h and against *S. aureus* for up to 5h [44]. Similar antibacterial activity has been depicted by the ECM of the caprine lung, caprine skin, porcine SIS, urinary bladder and liver tissue [44, 45, 50-53]. However, the exact mechanism of killing bacteria by ABPs is unknown [44, 52]. It has been suggested that ABPs may become directly attached with the bacterial cell membrane, causing membrane lysis, or diffuse into the bacterial cell cytoplasm, interfering with protein synthesis [44, 52]. If the decellularized caprine SIS is utilised as a biomaterial in skin tissue engineering, it will progressively break down *in-vivo* and constantly release antibacterial peptides, resulting in a prolonged antibacterial action in the host.

Assessment of hemocompatibility of the DG-SIS matrices showed no rupture of erythrocytes in the tubes containing DG-SIS matrices, whereas the erythrocytes were ruptured in the positive control, as indicated by the reddish appearance of the supernatant, implying full-scale hemolysis. Moreover, the hemolysis (%) values of all DG-SIS matrices were less than 5%. Thus, all DG-SIS matrices can be considered as non-hemolytic and hemocompatible. Similar results were also explained earlier [48].

Biocompatibility is the most crucial feature of decellularized biomaterial for tissue engineering. According to various studies, several factors have been involved in the biocompatibility of a decellularized biomaterial, including decellularizing chemicals, time duration for decellularization, decellularizing chemical-remains after decellularization and ECM components (GAG, proteoglycans and collagen) remaining after decellularization [19-21, 24, 37]. FESEM images depict good cell adherence and proliferation over the decellularized DG-SIS matrices after 5 days of cell culture. Thus, the in vitro cellular behaviour study demonstrated that all the DG-SIS matrices were cytocompatible and could potentially regenerate skin tissue and can be used for other TE applications. However, DP4 shows a significant difference from DP3; it may be the effect of a higher concentration of the chemicals (SDS and TX-100) used for decellularization. Recently, Rashtbar et al. [40] decellularized ovine SIS as ECM based scaffold for tissue engineering. In their study, a lower concentration of chemicals (SDS and TX-100) was used for ovine SIS decellularization, to get non-toxic D-SIS with improved cell attachment and proliferation. Overall, the comparative outcomes of this study suggested that the DP4 is the most suitable among the four protocols for

G-SIS decellularization. Comparison among all the DPs, in tabular form, are shown in supplementary information 3.

Conclusions

Caprine SIS was decellularized successfully by previously described decellularization protocols (DP1, DP2 and DP3) and by using an in-house developed protocol (DP4). DP4, by using hypertonic KI and mild non-ionic detergent with gentle mechanical agitation at low temperature (4°C), was better in terms of preservation of ECM (i.e., GAG and proteoglycan content), cell viability and proliferation. The earlier reported DPs (DP1, DP2 and DP3), where SDS is utilized for cell rupture, had affected the native microarchitecture and ECM composition of the caprine SIS, and the resultant DG-SIS were less cytocompatible than those developed with our in-house developed protocol DP4. Decellularizing temperature (4°C), used in DP4, palys a vital role in preservation of available ECM components in DG-SIS as compared to higher decellularization temperature (37°C) used in other DPs. DG-SISs were found to be fibrous, hemocompatible, cytocompatible, hydrophilic and biodegradable. The DG-SIS also showed good mechanical properties and hence, may be potentially utilized for various TE applications. Good viability and proliferation of the L929 fibroblast cells, on the DG-SIS, suggests its suitability in skin TE. Furthermore, DG-SIS can be converted into different forms (powder, gel and sponge/scaffold) and can be modified with various polymers, herbal drugs and nanomaterial to improve the properties for various tissue engineering applications. Antibacterial peptides which are produced during the degradation of SIS scaffold-matrix, when implanted in the patient's body, will protect the cells from bacterial infections. Repairing of external skin injury may become difficult due to bacterial infection: in that case, if caprine SIS is used for skin regeneration, it will gradually degrade and release antibacterial peptides continuously, providing a sustained antibacterial effect in the host. During surgery for the treatment of skin tissues, bacterial infection may also occur. And, in that case also, if caprine SIS is used as a biomaterial, it will provide antibacterial effect in the host. In future, ECM of DG-SIS may be converted into ECM ink for 3D printing and utilized in different fields of biomedical science.

Declaration of Competing Interests

The authors declare that they have no known competing financial interests or personal relationships that could have appeared to influence the work reported in this paper.

Acknowledgements

To support this research, the authors acknowledge the Indian Institute of Technology Roorkee and the National Institute of Technology Rourkela, India.

Supplementary materials

Supplementary material associated with this article can be found, in the online version, at doi:10.1016/j.bbiosy.2021.100035.

References

[1] Vacanti JP, Langer R. Tissue engineering: the design and fabrication of living replacement devices for surgical reconstruction and transplantation. Lancet 1999;354:32–4.
[2] Gautam S, Ambwani S. Tissue engineering: new paradigm of biomedicine. Biosci Biotechnol Res Asia 2019;16:521–32.
[3] Wu I, Elisseeff J. Biomaterials and tissue engineering for soft tissue reconstruction. natural and synthetic biomedical polymers. Elsevier; 2014. p. 235–41.
[4] Purohit SD, Bhaskar R, Singh H, et al. Development of a nanocomposite scaffold of gelatin–alginate–graphene oxide for bone tissue engineering. Int J Biol Macromol 2019;133:592–602.
[5] Hussey GS, Keane TJ, Badylak SF. The extracellular matrix of the gastrointestinal tract: A regenerative medicine platform. Nat Rev Gastroenterol Hepatol 2017;14:540–52.
[6] Purohit SD, Singh H, Bhaskar R, et al. Fabrication of Graphene Oxide and Nanohydroxyapatite Reinforced Gelatin–Alginate Nanocomposite Scaffold for Bone Tissue Regeneration. Front Mater 2020;7:1–10.
[7] Gautam S, Sharma C, Purohit SD, et al. Gelatin-polycaprolactone-nanohydroxyapatite electrospun nanocomposite scaffold for bone tissue engineering. Mater Sci Eng C 2021;119:111588.
[8] Purohit SD, Singh H, Bhaskar R, et al. Gelatin—alginate—cerium oxide nanocomposite scaffold for bone regeneration. Mater Sci Eng C 2020;116:111111.
[9] Ali A, Bano S, Poojary SS, et al. Effect of incorporation of montmorillonite on Xylan/Chitosan conjugate scaffold. Colloids Surfaces B Biointerfaces 2019;180:75–82.
[10] Kohane DS, Langer R. Polymeric Biomaterials in Tissue Engineering. Pediatric research 2008;63:487–91.
[11] Bhatia SK. Biomaterials for clinical applications (Google eBook). Springer Science & Business Media NY, USA; 2010. ISBN: 978-1-4419-6919-4. DOI: 10.1007/978-1-4419-6920-0.
[12] Keane TJ, Saldin LT, Badylak SF. Decellularization of mammalian tissues preparing extracellular matrix bioscaffolds. Characterization and design of tissue scaffolds. Woodhead Publishing; 2016. p. 75–103.
[13] Gupta SK, Dinda AK, Potdar PD, et al. Fabrication and characterization of scaffold from cadaver goat-lung tissue for skin tissue engineering applications. Mater Sci Eng C 2013;33:4032–8.
[14] Capella-Monsonís H, Tilbury MA, Wall JG, DI Zeugolis. Porcine mesothelium matrix as a biomaterial for wound healing applications. Materials Today Bio 2020;7:100057.
[15] Luo JC, Chen W, Chen XH, et al. A multi-step method for preparation of porcine small intestinal submucosa (SIS). Biomaterials 2011;32:706–13.
[16] Cramer MC, Badylak SF. Extracellular matrix-based biomaterials and their influence upon cell behaviour. Ann Biomed Eng 2020;48:2132–53.
[17] Capella-Monsonís H, DI Zeugolis. Decellularized xenografts in regenerative medicine: from processing to clinical application. Xenotransplantation 2021;12:e12683.
[18] Capella-Monsonís H, De Pieri A, Peixoto R, et al. Extracellular matrix-based biomaterials as adipose-derived stem cell delivery vehicles in wound healing: a comparative study between a collagen scaffold and two xenografts. Stem cell Res Ther 2020;11(1):1–15.
[19] Saldin LT, Cramer MC, Velankar SS, et al. Extracellular matrix hydrogels from decellularised tissues: Structure and function. Acta Biomater 2017;49:1–15.
[20] Paulo Zambon J, Atala A, Yoo JJ. Methods to generate tissue-derived constructs for regenerative medicine applications. Methods 2020;171:3–10.
[21] Gilpin A, Yang Y. Decellularization strategies for regenerative medicine: from processing techniques to applications. Biomed Res Int 2017 2017: ID 9831534.
[22] Xu H, Xu B, Yang Q, et al. Comparison of decellularization protocols for preparing a decellularized porcine annulus fibrosus Scaffold. PloS one 2014;9(1):e86723.
[23] García-Gareta E, Abduldaiem Y, Sawadkar P, et al. Decellularised scaffolds: just a framework? Current knowledge and future directions. J Tissue Eng 2020;11:2041731420942903.
[24] Mendibil U, Ruiz-Hernandez R, Retegi-Carrion S, et al. Tissue-specific decellularization methods: rationale and strategies to achieve regenerative compounds. Int J Mol Sci 2020;21:1–29.
[25] Roosens A, Somers P, De Somer F, et al. Impact of detergent-based decellularization methods on porcine tissues for heart valve engineering. Ann Biomed Eng 2016;44:2827–39.
[26] Liao J, Xu B, Zhang R, et al. Applications of decellularised materials in tissue engineering: advantages, drawbacks and current improvements, and future perspectives. J Mater Chem B 2020;8:10023–49.
[27] Chen G, Kawazoe N. Decellularization techniques for preparation of decellularized extracellular matrices in tissue engineering applications. Encycl Anal Chem 2019:1–15.
[28] Buckenmeyer MJ, Meder TJ, Prest TA, et al. Decellularization techniques and their applications for the repair and regeneration of the nervous system. Methods 2020;171:41–61.
[29] Hillebrandt KH, Everwien H, Haep N, et al. Strategies based on organ decellularization and recellularization. Transpl Int 2019;32:571–85.
[30] Oliveira AC, Garzón I, Ionescu AM, et al. Evaluation of small intestine grafts decellularization methods for corneal tissue engineering. PLoS One 2013;8(6):e66538.
[31] Keckler SJ, Spilde TL, St Peter SD, et al. Treatment of bronchopleural fistula with small intestinal mucosa and fibrin glue sealant. Ann Thorac Surg 2007;84:1383–6.
[32] Fiala R, Vidlar A, Vrtal R, et al. Porcine small intestinal submucosa graft for repair of anterior urethral strictures. Eur Urol 2007;51:1702–8.
[33] Moreira Lemos NL de B, Kamergorodsky G, Antunes Faria AL, et al. Small intestinal submucosa patch for extensive vaginal endometriosis resection. J Minim Invasive Gynecol 2009;16:765–7.
[34] Agarwal T, Maiti TK, Ghosh SK. Decellularized caprine liver-derived biomimetic and pro-angiogenic scaffolds for liver tissue engineering. Mater Sci Eng C 2019;98:939–48.
[35] Singh H, Purohit SD, Bhaskar R, et al. Biomatrix from goat-waste in sponge/gel/powder form for tissue engineering and synergistic effect of nanoceria. Biomed Mater 2021;16(2):025008.
[36] Saldin LT, Cramer MC, Velankar SS, et al. Extracellular matrix hydrogels from decellularised tissues: structure and function. Acta Biomater 2017;49:1–15.
[37] Syed O, Walters NJ, Day RM, et al. Evaluation of decellularization protocols for production of tubular small intestine submucosa scaffolds for use in oesophageal tissue engineering. Acta Biomater 2014;10:5043–54.
[38] Parmaksiz M, Elcin AE, Elcin YM. Decellularization of bovine small intestinal submucosa and its use for the healing of a critical-sized full-thickness skin defect, alone

and in combination with stem cells, in a small rodent model. J Tissue Eng Regen Med 2017;11:1754–65.
[39] Farrokhi A, Pakyari M, Nabai L, et al. Evaluation of detergent-free and detergent-based methods for decellularization of murine skin. Tissue Eng Part A 2017;24(11-12):955–67.
[40] Rashtbar M, Hadjati J, Ai J, et al. Characterization of decellularized ovine small intestine submucosal layer as extracellular matrix-based scaffold for tissue engineering. J Biomed Mater Res - Part B Appl Biomater 2018;106:933–44.
[41] Manuelidis L, Liu Y, Mullins B. Strain-specific viral properties of variant Creutzfeldt–Jakob disease (vCJD) are encoded by the agent and not by host prion protein. J Cell Biochem 2009;106(2):220–31.
[42] Banerjee I, Mishra D, Das T, et al. Caprine (Goat) collagen: a potential biomaterial for skin tissue engineering. J Biomater Sci Polym Ed 2012;23(1-4):355–73.
[43] Vaccari G, Panagiotidis CH, Acin C, et al. State-of-the-art review of goat TSE in the European Union, with special emphasis on PRNP genetics and epidemiology. Veterinary research 2009;40(5):1–8.
[44] Gupta SK, Dinda AK, Mishra NC. Antibacterial activity and composition of decellularized goat lung extracellular matrix for its tissue engineering applications. Biol Eng Med 2017;2:1–7.
[45] Dhasmana A, Singh L, Roy P, Mishra NC. Honey incorporated antibacterial acellular dermal matrix for full-thickness wound healing. angiogenesis 2018;1:8–10 https://apeda.gov.in/apedawebsite/SubHead_Products/Sheep_Goat_Meat.htm.
[46] Farndale RW, Buttle DJ, Barrett AJ. Improved quantitation and discrimination of sulphated glycosaminoglycans by use of dimethylmethylene blue. Biochim Biophys Acta (BBA)-Gen Sub 1986;883:173–7.
[47] Fan MR, Gong M, Da LC, et al. Tissue engineered oesophagus scaffold constructed with porcine small intestinal submucosa and synthetic polymers. Biomed Mater 2014;9(1):015012 2014.
[48] Shi L, Ronfard V. Biochemical and biomechanical characterization of porcine small intestinal submucosa (SIS): a mini review. Int J Burn Trauma 2013;3:173–9.
[49] Brennan EP, Reing J, Chew D, et al. Antibacterial activity within degradation products of biological Scaffolds composed of extracellular matrix. Tissue Eng 2006;12(10):2949–55.
[50] Sarikaya A, Record R, Wu CC, Tullius B, Badylak S, et al. Antimicrobial activity associated with extracellular matrices. Tissue Eng 2002;8:63–71.
[51] Boman HG. Peptide antibiotics and their role in innate immunity. Annu Rev Immunol 1995;13:61–92.
[52] Boman HG, Agerberth B, Boman A. Mechanisms of action on Escherichia coli of cecropin P1 and PR-39, two antibacterial peptides from pig intestine. Infect Immun 1993;61:2978–84.
[53] Singh H, Purohit SD, Bhaskar R, et al. Curcumin in decellularized goat small intestine submucosa for wound healing and skin tissue engineering. J. Biomed. Mater. Res. Part B Appl. Biomater. 2021:1–10.